RESEARCH ARTICLE
doi: 10.2306/scienceasia1513-1874.2021.072

ScienceAsia 47 (2021): **556–566**

Apoptotic induction of the water fraction of *Pseuderanthemum palatiferum* ethanol extract powder in Jurkat cells monitored by FTIR microspectroscopy

Benjawan Dunkhunthod[a], Benjamas Chiraatthakit[a], Benjamart Chitsomboon[b], Ratana Kiatsongchai[b], Kanjana Thumanu[c], Sumalee Musika[d], Patcharawan Sittisart[e,*]

[a] Institute of Science, School of Preclinic, Suranaree University of Technology, Nakhon Ratchasima 30000 Thailand
[b] Institute of Science, School of Biology, Suranaree University of Technology, Nakhon Ratchasima 30000 Thailand
[c] Synchrotron Light Research Institute (Public Organization), Nakhon Ratchasima 30000 Thailand
[d] Faculty of Sciences and Liberal Arts, Department of Applied Biology, Rajamangala University of Technology Isan, Nakhon Ratchasima 30000 Thailand
[e] Faculty of Liberal Arts and Science, Division of Environmental Science, Sisaket Rajabhat University, Sisaket 33000 Thailand

*Corresponding author, e-mail: patcwan07@gmail.com

Received 12 Nov 2020
Accepted 13 Jun 2021

ABSTRACT: *Pseuderanthemum palatiferum* (Nees) Radlk. is one of the most commonly used medicinal plants in Thailand for treatment of many diseases including cancer. In this study, we investigated the effect of the water fraction of *Pseuderanthemum palatiferum* ethanol extract powder (WEP) on apoptosis induction in Jurkat cells, and Fourier-transform infrared (FTIR) microspectroscopy was applied to determine biomolecular changes in apoptotic cell death. GC-MS analysis revealed that the major constituents in the extract were 4-Vinylphenol (35.71%), 2-Methoxy-4-vinylphenol (12.12%), 4H-pyran-4-one, 2,3-dihydro-3,5-Dihydroxy-6-methyl- (10.93%), 1-Dodecanlol (6.72%), and Dodecyl acrylate (4.34%). Many other compounds were also detected, but their contents were small. WEP showed selective cytotoxicity to Jurkat cells, while minimal toxicity to normal peripheral blood mononuclear cells (PBMCs) was observed. WEP also induced apoptotic cell death in Jurkat cells as evidenced by the morphological changes, DNA ladder formation, and the release of cytochrome C. FTIR analysis revealed changes of macromolecules with increased intensity of lipid region and decreased intensity of nucleic acid region. Thus, the results confirmed apoptotic induction of WEP against Jurkat cells. This study suggests that a combination of classical biological method and FTIR microspectroscopy could successfully detect biochemical and biophysical features of apoptosis in Jurkat cells.

KEYWORDS: *Pseuderanthemum palatiferum*(Nees) Radlk, Jurkat cells, apoptosis, FTIR microspectroscopy

INTRODUCTION

Leukemia is a worldwide common hematologic malignancy with approximately 437 033 new cases (2.4% of all cancer cases) and 309 006 deaths (3.2% of all cancer deaths) [1]. Treatment for leukemia depends on individual's age, cancer type, and severity of the disease. In most cases, chemotherapy is the first line of treatment for this disease. Despite its success, chemotherapy is often impeded by chemotherapeutic resistance of cancer cells, failure of target specificity, and adverse effects. For the past decade, researchers have discovered new drugs for improving the treatment of T-cell leukemia. Jurkat cells are an immortalized human T lymphocyte cell line originally established from peripheral blood of a 14-year-old boy with relapsed acute lymphoblastic leukemia (ALL) [2]. The Jurkat cell line has been the most often used as acute T cell leukemia to verify the therapeutic potential of anti-cancer compounds [3–5]. Throughout history, plants have been valuable sources for novel anti-cancer drugs [6]. Several studies have described the beneficial effects of plant extract on the risk reduction of chronic diseases, including cancer [7–9]. *Pseuderanthemum palatiferum* (Nees) Radlk. (*P. palatiferum*), a member of Acanthaceae family, is known as a rich source of multiple types of potent antioxidants: polypheno-

lic acids, flavonoids, gallic acid, tannic acid, catechin, rutin, isoquercetin, quercetin, kaempferol, β-sitosterol, and stigmasterol as well as other potential anticancer agents [10, 11]. Biological properties of *P. palatiferum* have been characterized including antioxidant, antidiabetic, anti-inflammatory, hypotensive, and anticancer activities [8–13]. Previous studies showed that *P. palatiferum* extract exhibited anti-proliferative effects on 3 types of colon cancer cell lines: HCT15, SW48, and SW480 [14]; and the fresh leaf ethanolic extract of the plant induced MDA-MB-231 human breast cancer programmed cell death [8]. The aqueous *P. palatiferum* leaf extracts also exerted anti-cancer activity by suppression of cell viability and induction of ROS mediated mitochondrial dependent apoptosis in A549 human lung cancer cells [15].

Recently, Fourier-transform infrared (FTIR) microspectroscopy was used as a label-free technique to monitor cancer cell apoptosis and to understand the spectral fingerprints of apoptotic cells. FTIR spectroscopy is a non-destructive technique, a major advantage that can provide biochemical profiles in a cell population within a few seconds. The objective of this study was to investigate the effect of water fraction of *P. palatiferum* ethanol extract powder (WEP) on the induction of apoptosis in Jurkat cell lines using both classical biological assay and FTIR microspectroscopy.

MATERIALS AND METHODS

Chemicals and reagents

3-(4,5-Dimethylthiazol-2-yl)-2, 5-diphenyltetrazolium bromide (MTT), Roswell Park Memorial Institute (RPMI1640) medium, and Dulbecco's Modified Eagle's medium (DMEM) were obtained from Gibco Invitrogen (Grand Island, NY, USA). Fetal bovine serum (FBS) was obtained from Hyclone (Logan, UT, USA). All other reagents were purchased from Sigma-Aldrich Co. (St. Louis, MO, USA).

Plant material

P. palatiferum was purchased from a garden in Yasothon Province, Thailand. It was authenticated with a voucher specimen number of "BKF 174009" by Dr. Kongkanda Chayamarit, the Royal Forest Department and deposited at the herbarium of Department of Royal Forest, Bangkok, Thailand.

Preparation of the water fraction of *P. palatiferum* ethanol extract

The preparation of crude *P. palatiferum* leaf extracts was as described [13]. Briefly, fresh leaves (4 kg) of *P. palatiferum* were blended in 16 l of 95% ethanol and filtered through a gauze. The extract was centrifuged, filtered, concentrated using a vacuum rotary evaporator (Buchi Labortechnik AG, Flawil, Switzerland), and dried by lyophilization (FreezeZone 12 plus, Labconco Corp., MO, USA) into powder. Then, the powder of 95% ethanol crude extract was partitioned between hexane and water (1:1, v/v). The water fraction was collected, centrifuged, filtered, evaporated, and lyophilized to obtain the water fraction of *P. palatiferum* ethanol extract powder (WEP).

GC-MS analysis

The GC-MS analysis of bioactive compounds from WEP was done using a Bruker 450-GC/Bruker320-MS equipped with Rtx-5MS fused silica capillary column (30 m × 0.25 mm; 0.25 μm in the thickness of film). Fifty micrograms of WEP was dissolved in 1 ml of methanol and filtered through syringe filter with a 0.45 μm pore size. Two μl of WEP was injected in a split mode (1:5) with helium as the carrier gas at 1 ml/min. Spectroscopic detection by GC-MS involved an electron ionization system utilizing high energy electrons (70 eV). The initial temperature was set at 50–215 °C with increasing rate of 5 °C/min for 33 min. Finally, the temperature was increased to 250 °C at 15 °C/min. The total running time of the GC was 51.5 min. The mass spectra were obtained by a scan mode of the mass range from 35 to 500 atomic mass units. Interpretation of the GC-MS mass spectra were made by using NIST mass spectral library 2008. Relative quantity of the chemical compounds present in WEP was expressed as percentage based on peak area produced in the chromatogram.

Cell culture

MCF-7 (human breast adenocarcinoma cell line) and PC-3 (human prostate adenocarcinoma cell line) were purchased from American Type Culture Collection (ATCC, USA). Jurkat leukemic cell line was purchased from Cell Line Services, Germany. Human normal peripheral blood mononuclear cells were kindly provided by Blood Bank of Maharat Nakhon Ratchasima Hospital, Nakhon Ratchasima Province, Thailand. MCF-7 cells were cultured in DMEM with high glucose. Jurkat cells, PC-3, and

PBMCs cells were cultured in RPMI1640 medium. All complete media were supplemented with 10% FBS, 100 U/ml penicillin, and 100 μg/ml streptomycin. All cell lines were maintained at 37 °C in 5% CO_2 and 95% humidity.

Isolation of normal peripheral blood mononuclear cells (PBMCs)

Buffy coat was isolated by Biocoll separating solution, density 1.077 g/ml. Briefly, the whole blood was diluted with an equal volume of phosphate buffer saline (PBS). The diluted solution was carefully laid onto the Biocoll separating solution and centrifuged at $400 \times g$ for 30 min at 25 °C. The PBMC layer was collected and washed twice with PBS. This study was approved by the Ethics Committee for Researches Involving Human Subjects (in case of minimal risk review) of Suranaree University of Technology (Project code: EC-57-04).

In vitro cytotoxic test (MTT assay)

The cytotoxic effect of WEP on cell proliferation was determined by MTT assay [16]. Briefly, the cells were seeded in a 96-well plate at a density of 2×10^4 cells/well for PC-3 and 2.5×10^4 cells/well for MCF-7. The cells were allowed to adhere overnight, and then treated with various concentrations of WEP for 24 h. The Jurkat cells and the PBMCs were seeded at a density of 2.5×10^4 and 2×10^6 cells/well, respectively, and then treated with various concentrations of WEP for 24 h. After incubation, the cell viability was evaluated by MTT assay. The percentage of cell viability was calculated as follows: the percentage of cell viability = (absorbance of the test group/absorbance of the control group) × 100.

DNA fragmentation

Jurkat cells were seeded at a density of 1.875×10^6 cells/dish in a 100 mm^2 culture dish. The cells were treated with 100, 300, and 600 μg/ml of WEP for 24 h, or treated with 300 μg/ml of WEP for 6, 12, and 24 h. Etoposide (40 μg/ml) was used as positive control. After treatment, the cells were collected, washed twice with PBS, and extracted using QIAamp DNA Mini Kit (QIAGEN, Germany). Five micrograms of DNA samples in AE buffer were mixed with 100 μg/ml RNase A and incubated at 37 °C for 30 min. DNA samples were loaded on 1.5% agarose gel and electrophoresed at 70 volts for 1.50 h. After that, the gel was stained with 0.5 μg/ml ethidium bromide and visualized under ultraviolet light (WEALTEC, Corp., NV, USA).

Hoechst 33258 staining

Nuclear morphological changes as a late marker of apoptosis were observed by staining the DNA with Hoechst 33258. Jurkat cells were seeded at a density of 5×10^5 cells/well in a 6-well plate. After WEP treatment, Jurkat cells were collected, washed twice with PBS, and fixed with 200 μl of ρ-formaldehyde (4%, v/v) for 20 min. Then, the cells were washed with PBS and further stained with 10 μg/ml Hoechst 33258 for 30 min at room temperature in the dark. The stained cells were washed with PBS and visualized under the inverted fluorescence microscope (Olympus IX51, Olympus Corp., Japan).

Annexin V-PI staining

The Annexin V-PI staining was used to evaluate early and late apoptotic cells induced by WEP. Jurkat cells were seeded at a density of 5×10^5 cells/well in a 6-well plate. After WEP treatment, Jurkat cells were collected and washed twice with PBS. Then, cells were stained with Annexin V-FITC Apoptosis Detection Kit (EXBIO, Czech Republic) according to manufacturer's instructions and analyzed by a flow cytometer (Becton Dickinson Biosciences, NJ, USA).

Cytochrome C release

The release of cytochrome C from mitochondria is an important hallmark in apoptotic pathway. The levels of cytochrome C in mitochondria can be directly detected by probing with anti-cytochrome C-FITC and analyzed by flow cytometer. Jurkat cells were seeded at a density of 5×10^5 cells/well in a 6-well plate. After treatment with WEP, Jurkat cells were collected and washed twice with PBS. Then, cell pellets (1×10^6 cells in 200 μl of PBS) were stained using Millipore's FlowCellect™ Cytochrome C kit (Millipore Sigma, Burlington, MA, USA). The stained cells were analyzed by flow cytometry.

FTIR microspectroscopy

Jurkat cells were seeded at a density of 5×10^5 cells/well in a 6-well plate. After treatment with WEP, the cells were collected, washed twice with 0.85% NaCl, dropped onto low-e microscope slides (MirrIR, Kevley Technologies), and vacuum dried for 30 min in a desiccator to eliminate the excess water. Dried cells were kept in a desiccator until further analysis with FTIR.

FTIR spectra were recorded using FTIR microspectroscopy equipment at the Synchrotron Light Research Institute (Public Organization), Thailand.

FTIR spectra were acquired with a Bruker Vertex 70 spectrometer coupled with a Bruker Hyperion 2000 microscope (Bruker Optics Inc., Ettlingen, Germany) – equipped with a nitrogen cooled MCT (HgCdTe) detector with a 36 × IR. The spectra were obtained in the reflection mode covering spectral range of 4000–600 cm^{-1} using an aperture size of 50 μm × 50 μm with a resolution of 6 cm^{-1}. Each spectrum was collected at 64 scans. OPUS 7.2 software was used to acquire FTIR spectral data and control instrument systems.

The spectra of samples (3000–2800 cm^{-1} and 1800–850 cm^{-1}) were identified by Principal Component Analysis (PCA) using the Unscrambler 9.7 software (CAMO Software AS, Oslo, Norway). The spectra preprocessing was performed by second derivative transformations using Savitzky-Golay algorithm (nine smoothing points) and normalized with extended multiplicative signal correction (EMSC). Two-dimension score plot and loading plot were used to represent the different classes of data and relations among variables of the data sets, respectively. The integrated peak areas of samples were analyzed using OPUS 7.2 software with spectral ranges of 3000–2800 cm^{-1} (lipid region), 1750–1730 cm^{-1} (C=O ester from lipid), and 1300–850 cm^{-1} (nucleic acids and other carbohydrates region).

Statistical analysis

All statistical significance was determined by performing a One-way analysis of variance (ANOVA) with Tukey's analysis using SPSS (Statistics Package for the Social Sciences, Version 18). Values were considered statistically significant when $p < 0.05$, and data were representative of at least three independent experiments.

RESULTS

Extraction yield

Fresh leaves of *P. palatiferum* were extracted by 95% ethanol, then the powder of the extract was partitioned between hexane and water (1:1, v/v), giving the WEP fraction. WEP exhibited recovery percentages of 1.15% and 52.5% based on the original weight of fresh leaves and the 95% ethanol crude extract partitioned with hexane and water, respectively.

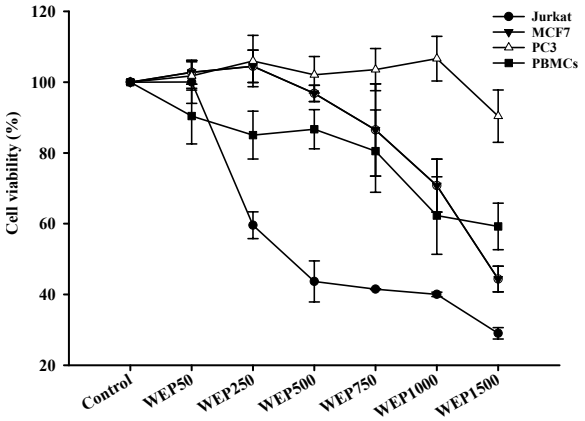

Fig. 1 Cytotoxic effect of WEP against different human cancer cell lines (PC-3, MCF-7, Jurkat cells) and normal human PBMCs. The cells were exposed to various concentrations of WEP for 24 h, then, assessed for cell viability by MTT assay. Reported means ± SD values ($n = 4$) are from a representative of three independent experiments.

GC/MS analysis of major volatile compounds obtained from WEP

The various volatile compounds present in WEP are shown in Table 1. The elution time, molecular formula, molecular weight (MW), and the relative amount in percentage of individual components were also presented. The major volatile substances present in WEP were 4-Vinylphenol (35.71%), 2-Methoxy-4-vinylphenol (12.12%), 4H-pyran-4-one, 2,3-dihydro-3,5-Dihydroxy-6-methyl- (10.93%), 1-Dodecanlol (6.72%), and Dodecyl acrylate (4.34%).

Anti-proliferative effects of WEP

The effect of WEP on the growth of three different human cancer cell lines (Jurkat, MCF-7, and PC-3 cell lines) and human normal PBMCs was evaluated by MTT assay. At 24 h, WEP showed concentration-dependent cytotoxicity on MCF-7, Jurkat, and PBMCs, but did not have cytotoxicity against PC-3 cell lines, as seen in Fig. 1. WEP exhibited the highest anti-proliferative effects against Jurkat cells with lowest IC_{50} value of 389.94 ± 13.26 μg/ml (Table 2). Importantly, the highest selectivity of WEP was observed in Jurkat cells with a selective index value of 3.6. These data were of interest, as they suggested that the extracts were more toxic to Jurkat cells than human normal PBMCs. Therefore, based on the most sensitive target of WEP, the Jurkat cells were selected for further investigation whether the cytotoxic effect of WEP was mediated through the apoptotic mechanism.

Table 1 GC-MS analysis of WEP.

No.	Compound name	Molecular formula	MW	RT (min)	% Area
1	2-Cyclopentene-1,4-dione	$C_5H_4O_2$	96.08	4.593	0.89
2	2-Furancarboxaldehyde, 5-methyl-	$C_6H_6O_2$	110.11	6.250	0.42
3	2,4-Dihydroxy-2,5-dimethyl-3(2H)-furan-3-one	$C_6H_8O_4$	144.12	6.592	1.42
4	Phenol	C_6H_6O	94.11	7.149	2.33
5	Benzenemethanol	C_7H_8O	108.14	8.177	1.87
6	Furaneol	$C_6H_8O_3$	128.13	8.999	2.01
7	Phenol, 2-methoxy-	$C_7H_8O_2$	124.14	9.523	0.51
8	2-Pyrrolidinone	C_4H_7NO	85.10	9.711	1.00
9	4H-Pyran-4-one, 2,3-dihydro-3,5-dihydroxy-6-methyl-	$C_6H_8O_4$	144.13	11.284	10.93
10	Methyl salicylate	$C_8H_8O_3$	152.15	12.391	3.75
11	4-Vinylphenol	C_8H_8O	120.15	13.474	35.17
12	2-Methoxy-4-vinylphenol	$C_9H_{10}O_2$	150.17	15.722	12.12
13	Phenol, 2,6-dimethoxy-	$C_8H_{10}O_3$	154.16	16.670	2.41
14	Phenol, 2-methoxy-4-(1-propenyl)-	$C_{10}H_{12}O_2$	164.20	19.150	0.62
15	1-Dodecanol	$C_{12}H_{26}O$	186.33	19.670	6.72
16	Megastigmatrienone	$C_{13}H_{18}O$	190.28	23.322	0.71
17	Dodecyl acrylate	$C_{15}H_{28}O_2$	240.38	24.675	4.34
18	Methoxyeugenol	$C_{11}H_{14}O_3$	194.23	25.015	0.81
19	Tetradecanoic acid	$C_{14}H_{28}O_2$	228.37	26.337	0.53
20	Vomifoliol	$C_{13}H_{20}O_3$	224.30	27.101	0.80
21	n-Hexadecanoic acid	$C_{16}H_{32}O_2$	256.42	30.351	1.89
22	Propanoic acid, 3-mercapto-, dodecyl ester	$C_{15}H_{30}O_2S$	274.46	31.167	3.80
23	Octadecanoic acid	$C_{18}H_{36}O_2$	284.48	33.894	0.78
24	Benzyl beta-d-glucoside	$C_{13}H_{16}O_7$	284.26	35.604	2.62
25	Benzyl beta-d-glucoside	$C_{13}H_{16}O_7$	284.26	36.584	1.57

Table 2 The IC_{50} values of extracts against different human cancer cell lines and human normal PBMCs.

Type of cell	IC_{50} (μg/ml) of WEP[†]	Selectivity index (SI)[‡]
Jurkat	389.94 ± 13.26^{a}	3.6
MCF-7	1434.45 ± 85.62^{b}	1.0
PC-3	$> 1500^{b}$	Cannot calculate
PBMCs	1431.03 ± 78.25^{b}	–

[†] Different letters within the same column are significantly different at $p < 0.05$.

[‡] To determine the cytotoxic selectivity of WEP, the selectivity index (SI) was calculated by IC_{50} of normal human PBMCs/IC_{50} of cancer cells.

WEP induced DNA fragmentation and nuclear morphological changes in Jurkat cells

The DNA fragmentation is used to detect DNA ladder at approximately 180–200 base pairs occurring when cells undergo apoptosis. The fragmented DNA was clearly observed in Jurkat cells after exposure to WEP in both concentration- and time-dependent manners, as shown in Fig. 2A. As expected, the DNA ladder formation was clearly observed in the positive control group (40 μg/ml etoposide) at 24 h of exposure.

The nuclear morphological changes of Jurkat cells after WEP treatment were observed by Hoechst 33258 staining. As seen in Fig. 2B, Jurkat cells exposed to WEP at 300 μg/ml demonstrated condensed and fragmented nuclei (white arrow) for 12 and 24 h. The condensed and fragmented nuclei were also observed in Jurkat cells after treatment with WEP at 600 μg/ml for 24 h. Similarly, the etoposide 40 μg/ml showed the typical apoptotic nuclear morphological changes, including condensed and fragmented nuclei (white arrow). As expected, non-treated cells showed normal nuclear morphology.

WEP induced apoptosis and cytochrome C release in Jurkat cells

Annexin V-PI assay was further performed to confirm the apoptotic cell death induced by WEP. Annexin V has a high affinity for phosphatidylserine translocating from the inner to the outer leaflet of the plasma membrane, which is occurring at the early stage of apoptotic process. The representative flow cytometry dot plots with double Annexin V-PI

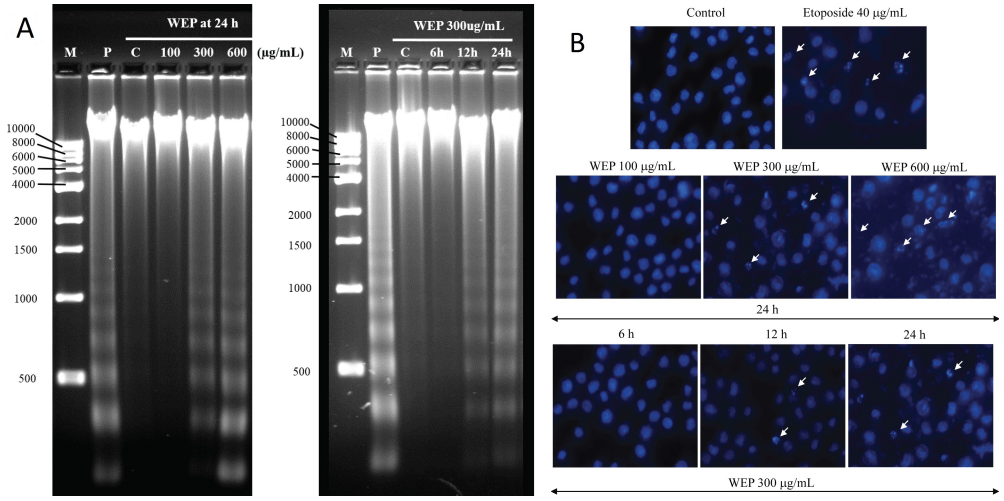

Fig. 2 DNA fragmentation (A) in Jurkat cells exposed to various concentrations of WEP for 24 h and indicated time points. Lane M, 1 kb DNA marker; lane P, positive control (40 μg/ml of etoposide); and lane C, control. Nuclear morphological changes (B) in Jurkat cells exposed to various concentrations of WEP for 24 h and indicated time points. The condensed or fragmented nuclei were indicated as white arrows (Magnified × 400).

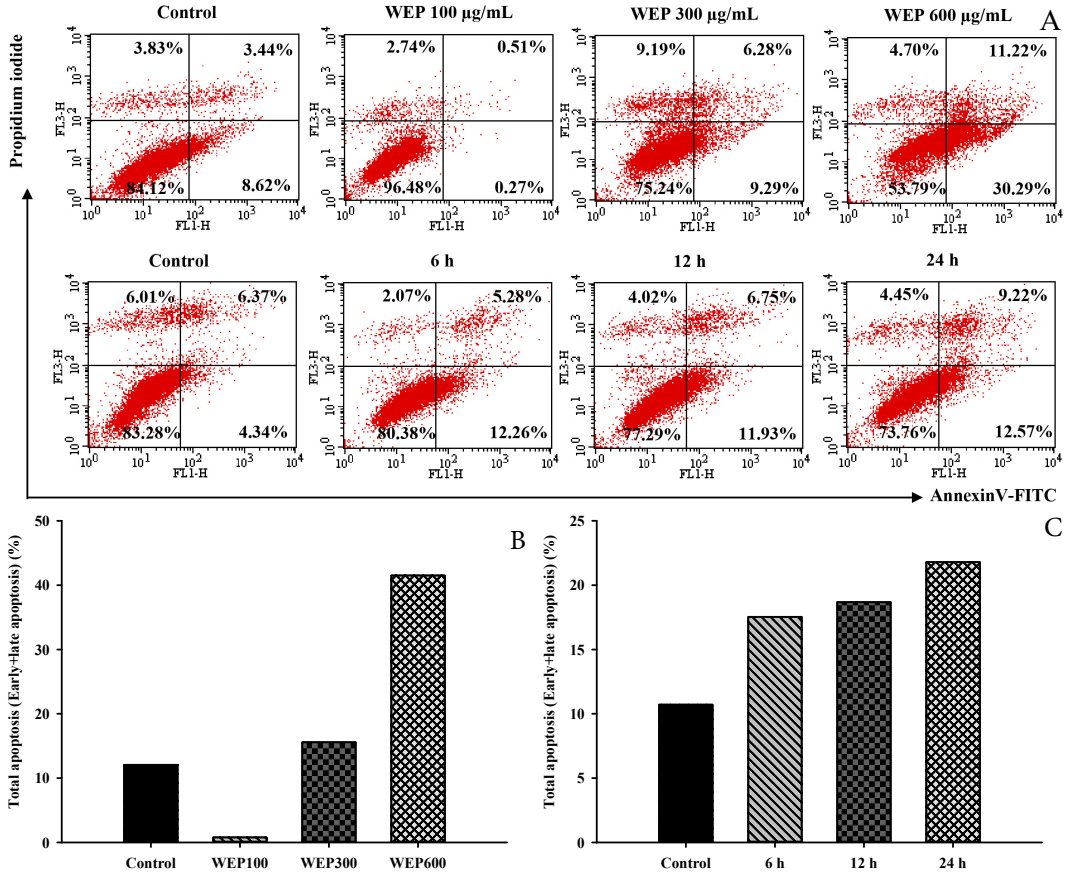

Fig. 3 Flow cytometric analysis of apoptosis in Jurkat cells. The representative flow cytometry dot plots with double Annexin V-PI staining (A). Bar charts show quantitative data of total apoptosis in cells exposed to various concentrations of WEP for 24 h (B) and kinetics of apoptosis induction in cells exposed to 300 μg/ml of WEP (C).

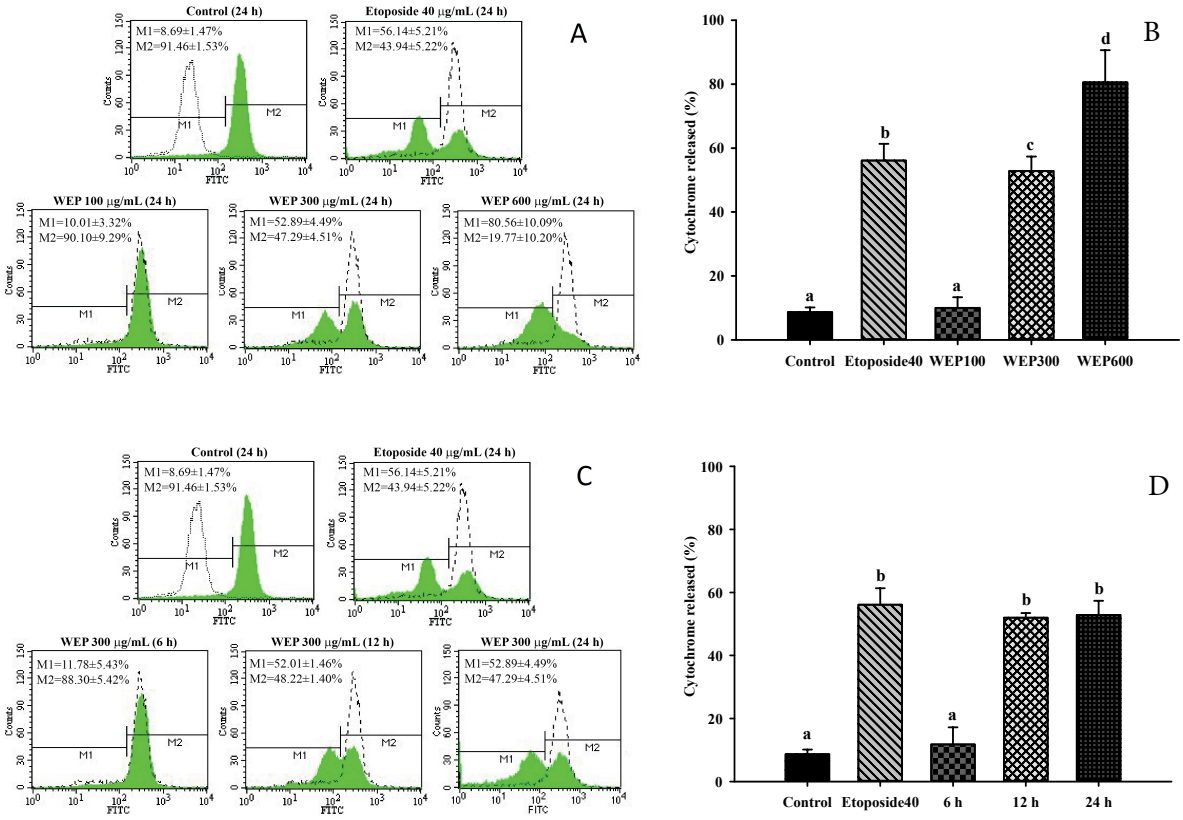

Fig. 4 Flow cytometry analysis of cytochrome C release of Jurkat cells exposed to various concentrations of WEP for 24 h (A and B) and kinetics of apoptosis induction in Jurkat cells exposed to 300 μg/ml of WEP (C and D). Left panel shows the representative of flow cytometry analysis of three independent experiments. M1 region shows the progressive increase of non-fluorescent cell population, and M2 region shows the decrease of highly fluorescent cell population. The reduction of fluorescent intensity in cell population implicates the release of cytochrome C from the mitochondria into the cytosol. Right panel represents the mean of percentages of cytochrome C release. Values are expressed as means ± SD ($n = 3$) of three independent experiments. Bars marked with different letters are significantly different at $p < 0.05$ as determined by one-way ANOVA with Tukey's post hoc test.

staining are shown in Fig. 3A. The total apoptosis (early + late apoptosis) of Jurkat cells treated with WEP increased gradually in both dose- and time-dependent manners as shown in Fig. 3B and Fig. 3C, respectively. WEP at 600 μg/ml for 24 h induced the highest total apoptosis rate of 41.51% in Jurkat cells.

The levels of cytochrome C in mitochondria can be directly detected by probing with anti-cytochrome C-FITC and analyzed by flow cytometer. As shown in Fig. 4A and Fig. 4B, the mitochondrial cytochrome C releases, compared with the untreated control cells, were dramatically increased by 6-fold and 9-fold after exposure to WEP at 300 and 600 μg/ml, respectively. Likewise, the time course study illustrated that the mitochondrial cytochrome C releases were significantly increased about 5-fold at both 12 and 24 h after exposure to 300 μg/ml of WEP, when compared with the control (Fig. 4CD).

FTIR microspectroscopy detected biomolecular changing of apoptotic cells

FTIR technique has been used to evaluate biomolecular changes of apoptotic cell death based on spectral information of cellular components. The band assignments of IR spectra of samples are summarized in Table 3. The original FTIR spectra are shown in Fig. 5A. The 2nd derivative spectra of the lipid region (3000–2800 cm^{-1}) and protein and nucleic acid region (1800–800 cm^{-1}) are shown

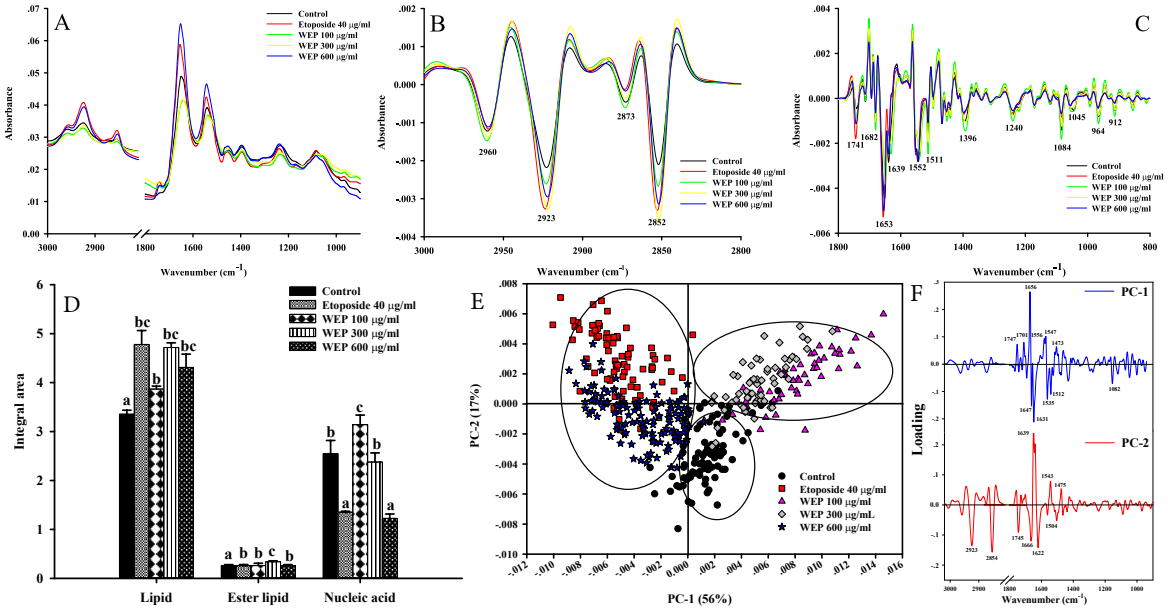

Fig. 5 Average original FTIR spectra (A) obtained from Jurkat control cells ($n = 90$) and exposed cells to WEP at 100 μg/ml ($n = 56$), 300 μg/ml ($n = 58$), 600 μg/ml ($n = 136$), and 40 μg/ml of etoposide positive control ($n = 84$) for 24 h. Average 2nd derivative spectra from experiment are represented in two regions: (B) lipid region (3000–2800 cm^{-1}) and (C) amide I protein and nucleic acid regions (1800–800 cm^{-1}). (D) shows the percentages of integrated areas for remarkable lipid, ester lipid, and nucleic acid regions. Data are represented as means ± SD for three replicates. Means with the same superscript are not significantly different from each other ($p < 0.05$). PCA analysis of FTIR spectral range 3000–800 cm^{-1} giving PCA score plot (E) and PCA loading plot (F).

Table 3 FTIR band assignments.

Band position 2nd derivative spectra (cm^{-1})	Band assignment
2923	C–H_2 antisymmetric stretch of methylene group of membrane phospholipids
2852	C–H_2 symmetric stretching: mainly lipids
1741	C=O stretching of lipid esters
1682	Amide I: β-turn
1653	Amide I: α-helix
1639	Amide I: β-pleated sheet
1240	PO_2-antisymmetric stretching vibrations: RNA, DNA and phospholipids
1084	PO_2-symmetric stretching vibrations: RNA, DNA
1045	C–O vibrations from glycogen and other carbohydrates
964	C–C vibrations from nucleic acids

in Fig. 5B and Fig. 5C, respectively. The spectral differences were observed in the mainly lipid region and nucleic acid and other carbohydrate regions. As seen in Fig. 5B, Jurkat cells after treatment with WEP or etoposide displayed a higher intensity of C–H stretching lipid bands (centered at 2923 cm^{-1} and 2852 cm^{-1}) and carbonyl lipid ester bands (1741 cm^{-1}) than the untreated cells. The nucleic acid intensity (centered at 1240 cm^{-1}, 1084 cm^{-1}, 1045 cm^{-1}, and 964 cm^{-1}) was decreased in 300 and 600 μg/ml of WEP- and 40 μg/ml of etoposide-treated group compared to the untreated cells. In contrast, Jurkat cells treated with WEP at 100 μg/ml for 24 h showed an increase in the intensity of nucleic acid absorbance.

Fig. 5D shows the average of integrated areas of lipid region (centered at 2971 cm^{-1}, 2950 cm^{-1}, 2936–2913 cm^{-1}, 2878–2867 cm^{-1}, and 2860–2845 cm^{-1}), ester lipid (centered at 1748–1733 cm^{-1}), and nucleic acid regions (1300–900 cm^{-1}). WEP-treated cells exhibited significant increase ($p < 0.05$) in the integrated area of lipid and ester lipid compared with untreated control cells. In contrast, the integrated areas of nucleic acid in Jurkat cells after treatment with WEP showed a dramatic decrease in dose-dependent manners. Moreover, Jurkat cells exposed to WEP at 600 μg/ml exhibited significant decrease ($p < 0.05$) in integrated areas of nucleic acid compared with untreated control cells.

Four clustering of spectra were clearly visualized in a two-dimensional PCA score plot (PC1 and PC2) as shown in Fig. 5E. The PCA loading plots exhibited the actual spectral changes between sample groups (Fig. 5F). PCA score plot demonstrated that the clusters of untreated cells and WEP-treated cells (100 and 300 μg/ml) were separated from the clusters of WEP-treated cells (600 μg/ml) and etoposide-treated cells along PC1 (56%). For WEP-treated cells (600 μg/ml) and etoposide-treated cells, the separation along PC1 can also be explained by having negative loadings in the spectral region centered at 1647 cm^{-1}, 1631 cm^{-1} (β-pleated sheet component), and 1082 cm^{-1} (nucleic acid (phosphodiester groups)). The spectra of the untreated-cells were also distinguished from WEP-treated cells (100 and 300 μg/ml) along PC2 (17%) by having negative loading PC2 in the C—H stretching region (centered at 2923 cm^{-1} and 2852 cm^{-1}) and C=O ester lipid (centered at 1745 cm^{-1}). The discrimination along PC2 between the negative score plot of spectra of Jurkat control cells and the positive score plot of spectra of WEP exposed cells at 100 and 300 μg/ml could be explained by positive loading of PC2 at 1639 cm^{-1} which indicated β-pleated sheet components.

DISCUSSION

P. palatiferum is widely used as a medicinal and ornamental plant in both Vietnam and Thailand. Several recent studies reported its biological activities of being antioxidant, antidiabetic [12], anti-inflammatory [11], hypotensive [10], hypoglycemic [17], and anti-proliferative [14].

In this study, we demonstrated distinct cytotoxic effects of WEP against various human cancer cell lines, with the highest cytotoxicity on Jurkat, followed by PC-3, and MCF-7 cell lines. This could be due to the selectivity of WEP in expressing the cytotoxic effect on different human cancer types. Different cancer cell lines with different genetic backgrounds responded differently to the same compound [18, 19]. Our results agreed with several previous reports which showed the cytotoxic effects of *P. palatiferum* crude extracts against various cancer cell lines including colon cancer, human breast cancer, and human lung cancer [12, 14]. Normal human PBMCs were used for studying the probable cytotoxicity of WEP against normal cells. The selectivity index (SI) values of WEP were calculated from the cytotoxicity of WEP against normal and cancer cells (Jurkat, MCF-7, and PC-3). The SI of 3.6 observed in Jurkat cells indicated that the cytotoxic effect of WEP towards the cancer cells was 3.6 times higher than the normal cells. Therefore, the most selective cytotoxicity of WEP was found in Jurkat cells with the highest SI values (3.6), and WEP also showed the highest cytotoxic effects on Jurkat cells with the lowest IC_{50} values (389.94 ± 13.26 μg/ml). Interestingly, certain properties of the cytotoxic effect observed in this study might be attributable to the presence of volatile compounds in WEP as indicated in Table 1. Among the 25 volatile compounds, 4-Vinylphenol and 2-Methoxy-4-vinylphenol had the property of anticancer activity [20, 21]. In CSC-enriched breast cancer cells, 4-Vinylphenol inhibited cancer stemness as well as suppressing metastatic activity [20]. 2-Methoxy-4-vinylphenol reduced the viability of Panc-1 cells and also suppressed the migratory activity of this cell line [21].

Cell death largely occurs through one of the two distinct processes: necrosis or apoptosis [22]. Consequently, it is necessary to distinguish apoptotic from necrotic cell death. Being the most sensitive target of WEP, Jurkat cells were selected for further investigation whether the cytotoxic effect of WEP was mediated through the apoptotic mechanism. The results indicated that WEP induced apoptotic cells death in Jurkat cells as evidenced by nuclear morphology changes, chromatin condensation, and DNA ladder formation. Flow cytometry analysis revealed that WEP induced apoptotic cell death with greater levels of early apoptosis, which was denoted by the flipping of phosphatidylserine to the extracellular surface of the cells. The phosphatidylserine externalization acts as a signal for macrophages to engulf the apoptotic cells [23]. To confirm apoptotic induction of WEP in Jurkat cells, the release of cytochrome C from mitochondria into the cytosol was further assessed. WEP-treated cells induced apoptosis with cytochrome C release from the mitochondria in both concentration- and time-dependent manners. The release of cytochrome C from mitochondria is a key initial step in the apoptotic process. During apoptosis, pro-apoptotic Bcl-2 family (Bax, Bad, and Bid) induce the permeabilization of outer mitochondrial membrane, and then cytochrome C and pro-apoptotic molecules are released into the cytosol. Cytochrome C binds to Apaf-1, instigates the assembly of the apoptosome, and induces caspase-dependent apoptotic pathway [24–26]. The results of our study indicated WEP-mediated apoptosis in Jurkat cells via the mitochondrial apoptotic pathway.

FTIR microspectroscopy was applied to mon-

itor biomolecular changes in WEP- treated cells. The FTIR spectra showed that WEP-treated cells had higher lipid content than the untreated cells. The increase in lipid absorbance of apoptotic cells may be related to membrane changes during apoptosis process, such as a collapse of lipid membrane asymmetry causing the inside out exposure of phosphatidylserine to the outer leaflet of membrane [27, 28]. In contrast, decreased lipid absorbance was found in necrotic cell death due to changes of membrane during necrosis, which included cell swelling and loss of plasma membrane integrity [29]. The nucleic acid content of WEP-treated Jurkat cells showed a dramatic decrease in a dose-dependent manner. These data are in accordance with the reports of many researchers, where the absorbance of nucleic acid region was decreased in apoptotic cell death, but increased in necrotic cells [30, 31]. The apoptotic DNA absorbed less IR due to the opaqueness of DNA (non-Beer-Lambert absorption) caused by condensation of DNA during apoptosis [32]. On the contrary, the DNA was completely unwound during necrosis; therefore, the necrotic DNA absorbed more IR than the DNA of apoptosis cells. In addition, the decreasing of DNA content may correlate with the progress of internucleosomal DNA cleavage during apoptosis process [33], which was related to the formation of DNA ladders as monitored by agarose gel electrophoresis. These findings proved that the FTIR technique is a good tool for the study of biochemical changes in WEP-treated Jurkat cells during apoptosis.

CONCLUSION

In conclusion, WEP exerted the most potent anti-proliferative effect against Jurkat cells, whereas less toxicity was observed in normal human PBMCs. The anti-proliferative effect of WEP was mediated via apoptotic induction in Jurkat cells. The FTIR analysis showed that the changing of biomolecules (lipid and nucleic acid) in WEP-treated cells may be related to the changing of plasma membrane structure and the internucleosomal DNA cleavage during apoptosis process. Therefore, FTIR microspectroscopy can be used as an alternative tool for studying the changing of biomolecules in apoptotic cells.

Acknowledgements: This study was financially supported by the National Research Council of Thailand (NRCT) through Suranaree University of Technology (SUT-104-53-36-09).

REFERENCES

1. Bray F, Ferlay J, Soerjomataram I, Siegel RL, Torre LA, Jemal A (2018) Global cancer statistics 2018: GLOBOCAN estimates of incidence and mortality worldwide for 36 cancers in 185 countries. *CA Cancer J Clin* **68**, 394–424.
2. Schneider U, Schwenk HU, Bornkamm G (1977) Characterization of EBVâĂŘgenome negative "null" and "T" cell lines derived from children with acute lymphoblastic leukemia and leukemic transformed non-Hodgkin lymphoma. *Int J Cancer* **19**, 621–626.
3. Wu JY, Tsai ET, Yang FY, Lin JF, Liao HF, Chen YJ, Kuo CD (2020) Inhibition of Jurkat T cell growth by N-farnesyl-norcantharimide through up-regulation of tumor suppressor genes and down-regulation of genes for steroid biosynthesis, metabolic pathways and fatty acid metabolism. *Anticancer Res* **40**, 2675–2685.
4. Moyo B, Mukanganyama S (2015) Antiproliferative activity of *T. welwitschii* extract on Jurkat T cells *in vitro*. *Biomed Res Int* **2015**, ID 817624.
5. Maioral MF, Bodack CM, Stefanes NM, Bigolin Á, Mascarello A, Chiaradia-Delatorre LD, Yunes RA, Nunes RJ, et al (2017) Cytotoxic effect of a novel naphthylchalcone against multiple cancer cells focusing on hematologic malignancies. *Biochimie* **140**, 48–57.
6. Habtemariam S, Lentini G (2018) Plant-derived anticancer agents: lessons from the pharmacology of geniposide and its aglycone, genipin. *Biomedicines* **6**, ID 39.
7. Buranrat B, Noiwetch S, Suksar T, Ta-ut A (2020) Inhibition of cell proliferation and migration by *Oroxylum indicum* extracts on breast cancer cells via Rac1 modulation. *J Pharm Biomed Anal* **10**, 187–193.
8. Komonrit P, Banjerdpongchai R (2018) Effect of *Pseuderanthemum palatiferum* (Nees) Radlk fresh leaf ethanolic extract on human breast cancer MDA-MB-231 regulated cell death. *Tumour Biol* **40**, 1–14.
9. Yang J, Tang X, Shuai L, Kwon YS, Kim MJ (2020) Chemical characterization, antioxidant properties and anti-inflammatory activity of Chinese water chestnut extracts. *ScienceAsia* **46**, 151–156.
10. Khonsung P, Panthong A, Chiranthanut N, Intahphuak S (2011) Hypotensive effect of the water extract of the leaves of *Pseuderanthemum palatiferum*. *J Nat Med* **65**, 551–558.
11. Sittisart P, Chitsomboon B, Kaminski NE (2016) *Pseuderanthemum palatiferum* leaf extract inhibits the proinflammatory cytokines, TNF-α and IL-6 expression in LPS-activated macrophages. *Food Chem Toxicol* **97**, 11–22.
12. Chayarop K, Peungvicha P, Wongkrajang Y, Chuakul W, Amnuoypol S, Temsiririrkkul R (2011) Pharmacognostic and phytochemical investigations of *Pseuderanthemum palatiferum* (Nees) Radlk. ex Lindau

leaves. *Pharmacogn J* **3**, 18–23.
13. Sittisart P, Chitsomboon B (2014) Intracellular ROS scavenging activity and downregulation of inflammatory mediators in RAW264.7 macrophage by fresh leaf extracts of *Pseuderanthemum palatiferum*. *Evid Based Complement Alternat Med* **2014**, ID 309095.
14. Pamok S, Vinitketkumnuen SSU, Saenphet K (2012) Antiproliferative effect of *Moringa oleifera* Lam. and *Pseuderanthemum palatiferum* (Nees) Radlk extracts on the colon cancer cells. *J Med Food* **6**, 139–145.
15. Kongprasom U, Sukketsiri W, Chonpathompikunlert P, Sroyraya M, Sretrirutchai S, Tanasawet S (2019) *Pseuderanthemum palatiferum* (Nees) Radlk extract induces apoptosis via reactive oxygen species-mediated mitochondria-dependent pathway in A549 human lung cancer cells. *Trop J Pharm Res* **18**, 287–294.
16. Sittisart P, Piakaew N, Chuea-Nongthon C, Dunkhunthod B (2019) Anti-proliferative and apoptosis-inducing activities of *Derris elliptica* (Roxb.) Benth. leaf extract on three human cancer cell lines. *Maejo Int J Sci Tech* **13**, 62–71.
17. Padee P, Nualkaew S, Talubmook C, Sakuljaitrong S (2010) Hypoglycemic effect of a leaf extract of *Pseuderanthemum palatiferum* (Nees) Radlk. in normal and streptozotocin-induced diabetic rats. *J Ethnopharmacol* **132**, 491–496.
18. Mai HD, Minh HN, Pham VC, Bui KN, Nguyen VH, Chau VM (2011) Lignans and other constituents from the roots of the Vietnamese medicinal plant *Pseuderanthemum palatiferum*. *Planta Med* **77**, 951–954.
19. Sak K (2014) Cytotoxicity of dietary flavonoids on different human cancer types. *Pharmacogn Rev* **8**, 122–146.
20. Leung HW, Ko CH, Yue GGL, Herr I, Lau CBS (2018) The natural agent 4-vinylphenol targets metastasis and stemness features in breast cancer stem-like cells. *Cancer Chemother Pharmacol* **82**, 185–197.
21. Kim DH, Han SI, Go B, Oh UH, Kim CS, Jung YH, Lee J, Kim JH (2019) 2-methoxy-4-vinylphenol attenuates migration of human pancreatic cancer cells via blockade of fak and akt signaling. *Anticancer Res* **39**, 6685–6691.
22. Majno G, Joris I (1995) Apoptosis, oncosis, and necrosis. An overview of cell death. *Am J Pathol* **146**, 3–15.
23. Wlodkowic D, Telford W, Skommer J, Darzynkiewicz Z (2011) Apoptosis and beyond: cytometry in studies of programmed cell death. *Methods Mol Biol* **103**, 55–98.
24. Donovan M, Cotter TG (2004) Control of mitochondrial integrity by Bcl-2 family members and caspase-independent cell death. *Biochim Biophys Acta* **1644**, 133–147.
25. Garrido C, Galluzzi L, Brunet M, Puig P, Didelot C, Kroemer G (2006) Mechanisms of cytochrome c release from mitochondria. *Cell Death Dis* **13**, 1423–1433.
26. Von AO, Renken C, Perkins G, Kluck RM, Bossy-Wetzel E, Newmeyer DD (2000) Preservation of mitochondrial structure and function after Bid-or Bax-mediated cytochrome c release. *J Cell Biol* **150**, 1027–1036.
27. Lamberti A, Sanges C, Arcari P (2010) FT-IR spectromicroscopy of mammalian cell cultures during necrosis and apoptosis induced by drugs. *Spectrosc* **24**, 535–546.
28. Wu BB, Gong YP, Wu XH, Chen YY, Chen FF, Jin LT, Cheng BR, Hu F, et al (2015) Fourier transform infrared spectroscopy for the distinction of MCF-7 cells treated with different concentrations of 5-fluorouracil. *J Transl Med* **13**, ID 108.
29. Liu KZ, Mantsch H (2001) Apoptosis-induced structural changes in leukemia cells identified by IR spectroscopy. *J Mol Struct* **565**, 299–304.
30. Machana S, Weerapreeyakul N, Barusrux S, Thumanu K, Tanthanuch W (2012) FTIR microspectroscopy discriminates anticancer action on human leukemic cells by extracts of *Pinus kesiya*; *Cratoxylum formosum* ssp. *pruniflorum* and melphalan. *Talanta* **93**, 371–382.
31. Zelig U, Kapelushnik J, Moreh R, Mordechai S, Nathan I (2009) Diagnosis of cell death by means of infrared spectroscopy. *Biophys J* **97**, 2107–2114.
32. Mohlenhoff B, Romeo M, Diem M, Wood BR (2005) Mie-type scattering and non-Beer-Lambert absorption behavior of human cells in infrared microspectroscopy. *Biophys J* **88**, 3635–3640.
33. Verrier S, Notingher I, Polak J, Hench L (2004) *In situ* monitoring of cell death using Raman microspectroscopy. *Biopolymers* **74**, 157–162.